ORIENTAL JOURNAL OF CHEMISTRY
An International Open Access, Peer Reviewed Research Journal

www.orientjchem.org

ISSN: 0970-020 X
CODEN: OJCHEG
2026, Vol. 42, No.(4):
Pg. 1471-1481

Structural Dissolution Behaviour of Phosphate-Silicate Glass Fertilizer Incorporating Calcined Red Gypsum for Controlled Release Fertilizer

FATIN 'AQILAH BINTI MAZLAN[1], MOHD FAIZ BIN HASSAN[1,2], MAZIDAH BINTI MAMAT[1,2] and MOHD AL AMIN BIN MUHAMAD NOR[1,2]*

[1]Faculty of Science and Marine Environment, Universiti Malaysia Terengganu, 21030 Kuala Nerus, Terengganu, Malaysia
[2]Advanced Nano Materials Research Interest Group (ANOMA), Faculty of Science and Marine Environment, Universiti Malaysia Terengganu, 21030 Kuala Nerus, Terengganu, Malaysia
Corresponding author E-mail: al_amin@umt.edu.my

http://dx.doi.org/10.13005/ojc/420421

(Received: June 17, 2026; Accepted: July 25, 2026)

ABSTRACT

Red gypsum (RG) is a major byproduct generated during titanium dioxide production in Malaysia. RG is rich in iron content and can cause environmental challenges due to large-scale disposal. This study investigates phosphate-silicate glass fertilizer with the addition of calcined red gypsum (CRG) replacing calcium oxide at 0 to 20 wt.%. Glass fertilizer is synthesized using conventional glass melting process with slow cooling and characterized with multi-technique. The addition of CRG into the glass matrix show a progressive increase of bulk density from 0.93 to 1.73 g/cm^3 and reduced apparent porosity from 37.4% to 20.7%. The formation of β-tricalcium and calcium silicate glass-ceramic phases is identified by XRD analysis with sharp peaks and crystalline phases. After 13-week dissolution testing, glass fertilizer with low addition of CRG content (0 to 5 wt.%) released nutrients rapidly, while glass fertilizer containing 10 to 20 wt.% CRG showed slower and more controlled release fertilizer. Despite all samples of glass fertilizer, the 10 wt.% CRG formulation showed the best overall analysis because of controlled K^+ release while Fe^{3+} and Al^{3+} sustained release within safe limits. These indicate that CRGs can effectively be added into phosphate-silicate glass fertilizer to achieve structural stability and valorize RG as a byproduct that is suitable for agricultural use.

Keyword: Calcined red gypsum, controlled-release fertilizer, dissolution behavior, glass fertilizer, industrial waste valorization.

INTRODUCTION

Fertilizers are important to agriculture for sustain high crop yields compared to conventional soluble fertilizers, which often have more negative effects. Leaching, runoff, and volatilization cause a significant amount of fertilizer loss due to the rapid dissolution of nutrient. Besides wasting money, this also causes major environmental issues, such as soil deterioration and eutrophication[1]. Controlled-release fertilizers (CRFs) are a new innovation to prevent this problem and also can release nutrients gradually in accordance with plant needs[2].

One potential kind of CRF is glass fertilizer. Essential macronutrients (K, P, Mg, S, Ca) and micronutrients (B, Fe, Mo, Cu, Zn, Mn) are incorporated into a silicate-based matrix. The beauty of glass fertilizers is that we can adjust the rate at which the nutrients are released by simply altering the composition of the glass, such as K_2O[3], Na_2O and K_2O [4] and Fe_2O_3 [5]. A layer of hydrated gel develops on the surface of the glass when it comes into contact with moisture. Next, nutrients are released by network dissolution and ion exchange, which is influenced by soil conditions, pH, and temperature[6]. Furthermore, high silica content may enhance stress tolerance of plants and can strengthen plant cell walls[7].

There is increasing interest in incorporating industrial byproducts into glass fertilizer production as part of circular economy principles. One such material is red gypsum (RG), an iron-rich byproduct of the sulfuric acid digestion of ilmenite during the production of titanium dioxide. Malaysia produced approximately 400,000 tons of RG, which is located in Kemaman, Terengganu, by Venator Asia Sdn Bhd [7]. RG mainly consists of calcium sulphate (~70 wt.%) and iron oxide (~30 wt.%), and it classified as scheduled waste (SW205) due to huge-scale stockpiling, and this raises concerns for sulphate leaching, soil acidification, heavy metal pollution, and health risks related to dust [8].

Calcining RG at 900^{0}C to removes water bound and turns hydrated calcium sulphate into anhydrous anhydrite to reduce leachability is a treatment for RG before use a secondary material in glass fertilizer. The addition of calcined red gypsum (CRG) in phosphate-silicate glass matrix makes the vitrification process prevents contaminants. The calcination process transformed RG into a valuable new product and addresses the waste problem.

RG has been explored in several studies by researchers such as applications in cement production[9], soil amendment[10], CO_2 capture[11], and catalysis[12], but RG incorporation in glass fertilizer systems remains unexplored by researchers. Therefore, the objectives of this study are to replace CaO with CRG at 0 to 20 wt.% in a phosphate-silicate glass fertilizer system, and to study how these substitutions affect glass structure, physical properties, and the kinetics of ion release. To the best of our knowledge, this is the first study to examine the purpose of CRG in phosphate-silicate glass fertilizer structure and dissolution testing for 13 weeks and as a potential for industrial byproduct valorization and designing controlled-release fertilizer.

MATERIALS AND METHOD

Red Gypsum Sampling and Preparation

RG was supplied from Venator Asia Sdn Bhd, Teluk Kalong, Kemaman, Terengganu, Malaysia. the RG sample was air-dried for 3 days and dried in an oven at 80^{0}C°Covernight to eliminate moisture. Then, RG was ground in a Planetary Ball Mill (PM100, Retsch GmbH, Germany) using a 10:1 ball-to-powder weight ratio at 250 rpm for one hour to obtain homogeneous particle sizes ≤63 μm. 50 g of ground RG was placed in an alumina (Al_2O_3) crucible and calcined at 900^{0}C with a heating rate 5°C/min, and two-hour holding period to complete phase transformation to anhydrous $CaSO_4$. The calcined red gypsum (CRG) was cooled to room temperature and immediately covered to prevent rehydration and contamination.

Preparation of Calcined Red Gypsum Glass Fertilizer (CRG-GF)

CRG-GF samples were synthesized using a conventional melt-derived glass technique followed by controlled slow cooling. A phosphate-silicate glass system with the general formula Na_2O-K_2O-(20-)CaO-CRG-Al_2O_3-SiO_2-P_2O_5 was developed, where represents the weight percentage of CRG substituting CaO at 0, 5, 10, 15, and 20 wt.%. The baseline composition (0% CRG) was adopted from Ersundu et al. (2022) as the control. Batch compositions were homogeneously mixed, charged

into alumina crucibles, and melted at 1300°C for one hour before cooling to room temperature. The chemical compositions of all CRG-GF samples are presented in Table 1.

Density and Porosity Measurements

Bulk density, apparent solid density, apparent porosity, and water absorption of CRG-GF samples were determined by Archimedes' principle in accordance with ASTM C373-14 [13]. Each sample was vacuum-dried for 30 minutes, weighed dry (D), fully saturated in distilled water for 24 hours, and then weighed suspended in water (S) and in saturated surface-dry condition (I). Equations [1] to [4] define the physical properties determined:

$$Bulk\ density\ \left(g/cm^3\right)=\frac{D}{I-S} \quad ....(1)$$

$$Apparent\ solid\ density\ \left(g/cm^3\right)=\frac{D}{D-S} \quad ....(2)$$

$$Apparent\ porosity\ (\%)=\frac{I-D}{I-S}\times 100\% \quad ....(3)$$

$$Water\ absorption\ (\%)=\frac{I-D}{D}\times 100\% \quad ....(4)$$

Characterization of CRG-GF

Fourier Transform Infrared Spectroscopy (FTIR)

Functional groups in CRG-GF samples were identified by ATR-FTIR spectroscopy using a Bruker Tensor 27 spectrometer equipped with a diamond ATR crystal. Spectra were collected over the wavenumber range 400-4000 cm^{-1} at a resolution of 4 cm^{-1} with 32 scans per spectrum.

X-ray Diffraction (XRD)

Phase composition was determined using a Rigaku SmartLab X-ray diffractometer operated at 40 kV and 30 mA. Finely ground CRG-GF powders were scanned over 2θ = 10°–80° at a scan rate of 2°/min with Cu Kα radiation. Phase identification was conducted using the ICDD PDF-2 database.

Scanning Electron Microscopy (SEM)

Surface and cross-sectional morphology of CRG-GF samples were examined using a Tescan Vega SEM operated at 15 kV. Samples were oven-dried at 60°C, mounted on aluminium stubs with carbon adhesive tape, and sputter-coated with gold to minimize charging effects. Imaging was performed at magnifications of 2000×.

Dissolution Study

Dissolution behaviour of CRG-GF was tested using static immersion, as reported by[3-5,14] which following a previous study of phosphate glass dissolution. 19.0 g of glass fertilizer sample immersed in 190 mL of deionized water using a solid-to-liquid ratio of 1:10 w/v for 13 weeks at 25 ± 2°C under static conditions. A calibrated Hanna Combo meter (HI 98129) was used to measure pH, electrical conductivity (EC), and total dissolved solids (TDS) every week. Measurements after 24-hour dissolution were also recorded. Before taking measurements, the bottles need to be shaken gently to ensure the homogeneity of sample.

ICP-OES Elemental Analysis

Ion potassium (K^+), aluminium (Al^{3+}), and iron (Fe^{3+}) concentrations in leachates were measured using Inductively Coupled Plasma Optical Emission Spectrometry (ICP-OES), PerkinElmer Avio 200. 0.45 μm syringe filters were used to filter aliquots (10 mL) and diluted as needed before analysis. A 100 mg/L multi-element ICP standard solution (Merck CertiPUR®, Cat No. 1.09492.0100). Every ICP-OES analysis was carried out in triplicate.

RESULTS AND DISCUSSION

Physical Observation of CRG-GF

Figure 1 shows the visual analysis of CRG-GF outer surfaces. The 0% CRG control showed a smooth, compact surface with few visible pores. Samples gradually showed more surface roughness and heterogeneity as the CRG level increased. The 20% CRG sample had a noticeably rough, porous, and darker texture that was consistent with a higher Fe_2O_3 content. Higher CRG levels resulted in progressively open, sponge-like microstructures with interconnected voids, whereas internal cross-sections shown in Figure 2 verified that the control was packed with few voids. A highly porous interior structure was seen at 20% CRG, which was explained by the evolution of SO_3 gas during melting as sulphate broke down at high temperatures.

Density and Porosity of CRG-GF

The physical characteristics of every CRG-GF composition are shown in Table 2. Bulk density increased progressively from 0.93 g/cm^3 (0% CRG) to 1.73 g/cm^3 (20% CRG), whereas apparent porosity dropped from 37.4% to 20.7%, and water absorption correspondingly diminished. These patterns signify progressive structural densification resulting from the integration of CaO and Fe_2O_3 from CRG, which improves network cross-linking and glass-phase stability during the melting and cooling process[15], producing denser matrices with fewer linked voids. The trend of densification corresponds with the microstructural features identified in the SEM analysis.

Microstructural and Morphological Observation by SEM analysis

Figure 3 shows SEM analysis at 2000× magnification for 5 sample of CRG-GF. Control sample (0% CRG) showed glassy fracture with small porosity, while 10% CRG sample showed features with crystalline structure. High-CRG compositions (15-20%) showed dense crystallinity with a few empty areas, indicating of glass-ceramic structure.

The trend of densification corresponds with the microstructural features identified in the SEM analysis. The microstructural evolution observed in SEM show the interconnected pores in the control (0% CRG) which allowed rapid ion release, and the isolated void (20% CRG) easy to trap nutrients. Therefore, 10% CRG shows the ideal balance with enabling slow, steady nutrient release over time which is an attribute of controlled-release fertilizer[14].

Fourier Transform Infrared Spectroscopy (FTIR) Analysis

Figure 4 shows FTIR spectra of CRG-GF samples with varying CRG content (0-20%). All spectra revealed absorption bands of the phosphate-silicate glass network. Table 3 shows the assignment of seven absorption regions (A-G) identified in CRG samples.

XRD Analysis

Figure 5 shows XRD analysis for CRG-GF with crystalline peak trend with increasing CRG

Table 1: Chemical composition (wt.%) of CRG-GF samples with varying calcined red gypsum (CRG) substituted with CaO

Sample	Na_2O	K_2O	CaO	CRG	Al_2O_3	SiO_2	P_2O_5
0% CRG	12.5	12.5	20	0	5	5	45
5% CRG	12.5	12.5	15	5	5	5	45
10% CRG	12.5	12.5	10	10	5	5	45
15% CRG	12.5	12.5	5	15	5	5	45
20% CRG	12.5	12.5	0	20	5	5	45

Note: CRG=calcined red gypsum; all values are in wt.%

Table 2: Physical Properties of CRG-GF Samples including Bulk Density, Apparent Density, Apparent Porosity, and Water Absorption

Sample Code	Bulk Density (g/cm3)	Apparent Solid Density (g/cm3)	Apparent Porosity (%)	Water Absorption (%)
0% CRG	0.9314	1.4883	37.4226	40.1802
5% CRG	1.2082	1.7910	32.5413	26.9334
10% CRG	1.2198	1.6865	27.6738	22.6880
15% CRG	1.3636	1.8164	24.9306	18.2833
20% CRG	1.7262	2.1779	20.7421	12.0159

content. All samples exhibited sharp diffraction peaks at 2θ = 22.6° (111), 27° (003/201), 32° (112), and 37° (202), corresponding to β-tricalcium phosphate (β-$Ca_3(PO_4)_2$) and calcium silicate ($CaSiO_3$) phases[9,22] .

XRD analysis confirmed the formation of glass-ceramic (β-tricalcium phosphate and calcium silicate) phases in all CRG-GF samples. These happen because of slow control cooling process that cause nucleation from CaO-SiO_2-P_2O_5 system with the addition of network modifier content[14,17]. As CRG increases, XRD peaks become sharper because of the higher CaO and Fe_2O_3 content, and this reduces the melt viscosity and structural rearrangement after the cooling process[23], resulting in glass fertilizer dissolved into the glass structure and becoming glass-ceramic.

pH, Electrical Conductivity (EC), and Total Dissolved Solids (TDS) of immersion CRG-GF Samples after 13-week Dissolution

Figure 6 shows the pH value of CRG-GF samples for dissolution at 13 weeks. In early week, week 1-3, all samples show a pH value decrease, indicating that ion reactions are leached from glass matrix from the solution[10]. After initial phases, the pH value became stable. However, CRG-GF samples with higher CRG content (10-20%) stabilized at low pH values and this indicates that the addition of CRG alters the dissolution behaviour toward higher acidity.

Figure 7 shows the value of electrical conductivity (EC) of CRG-GF samples for 13 weeks. All samples show a gradual increase in EC value, which indicates nutrient release. Samples with low CRG (0-5%) show maximum EC response with the control (0% CRG) exceeding 17,000 μS/cm and 5% CRG exceeding 15,000 μS/cm at week 13. The 10% CRG sample shows 12,000 μS/cm showing a linear and controlled release compared to lower CRG samples. High CRG samples (15-20%) show sharply decreased EC value.

Figure 8 shows the total dissolved solids (TDS) value, which mirrors the pattern of the EC graph. The control (0% CRG) showed over 8,000 ppm, while 5% CRG showed almost 7,500 ppm at week 13. The 10% CRG shows a moderate value of TDS 5,500 ppm which indicates a balance of

Table 3: Assignment of FTIR absorption bands identified in CRG-GF samples

Label	Wavenumber (cm^{-1})	Functional Group	Probable Compound	References
A	496.92	Si-O-Si bending vibration	Silicate network deformation	[6], [14]
B	564.38	P-O-P symmetric bending/ Ca-O stretching	Calcium phosphate units ($Ca_3(PO_4)_2$)	[16]
C	620.11	Al-O stretching/ SO42- bending vibration	Aluminosilicate and sulphate groups from red gypsum ($CaSO_4$)	[17]
D	730.99	O-P-O bending vibration	Phosphate tetrahedra linkage	[18]
E	793.63	Non-bridging oxygen (NBO) Si-O- stretching	Network modifier cations (Na^+, K^+, Ca^{2+}) disrupting Si-O-Si	[19]
F	974.04	Symmetric stretching of P-O and Si-O bonds	Phosphate and silicate structural units	[20]
G	1124.27	Asymmetric stretching of Si-O-Si and P-O bonds	Silicate and phosphate network ($(SiO_4)^{4-}$, $(PO_4)^{3-}$ tetrahedra)	[14], [21]

dissolution rate of nutrient release without over-leaching. High CRG samples (15-20% CRG) show the lowest TDS values, with 20% CRG showing almost 4,200 ppm.

Dissolution studies for 13 weeks in deionized water show the pattern of the graph is composition-dependent for pH, EC, and TDS values. The control (0% CRG) shows rapid ion release, while higher content of CRG (15-20%) shows slow and restricted release. 10% CRG demonstrated good performance, with moderate values of EC and TDS. Glass dissolution started at initial phases which alkali ions are leached from glass matrix substitute with ion H^+ from the solution showing the fast reaction of ion-exchange[11], next, the reaction of ion-exchange turns into diffusion-controlled dissolution from the formation of gel layer[7] Calcium oxide (CaO) has calcium ions (Ca^{2+}) that neutralize hydrogen ions (H^+). This process showed that addition of CRG give

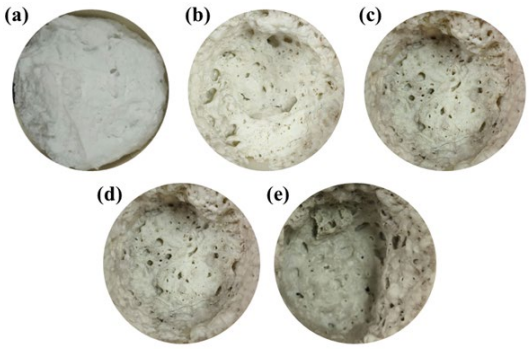

Fig. 1: Optical photographs of CRG-GF outer surfaces showing colour and texture evolution with increasing CRG content: (a) 0% CRG, (b) 5% CRG, (c) 10% CRG, (d) 15% CRG, and (e) 20% CRG

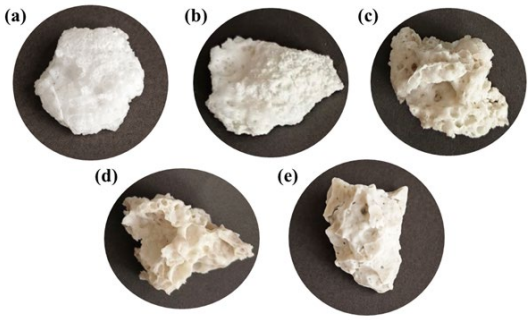

Fig. 2: Optical photographs of CRG-GF fractured cross-sections illustrating changes in internal porosity: (a) 0% CRG, (b) 5% CRG, (c) 10% CRG, (d) 15% CRG, and (e) 20% CRG

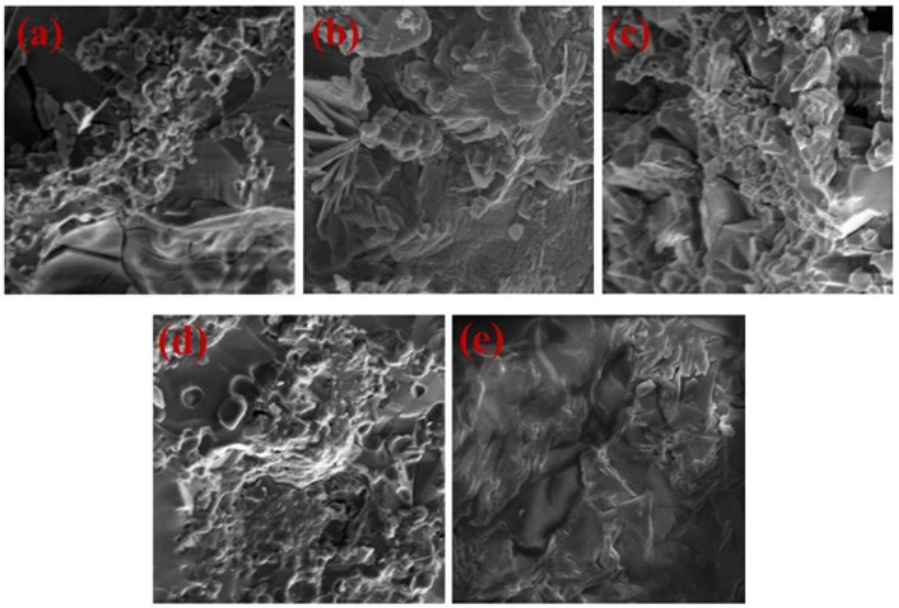

Fig. 3: SEM analysis (2000X) of CRG-GF fracture surfaces with different content of CRG (0-20%): (a) 0% CRG, (b) 5% CRG, (c) 10% CRG, (d) 15% CRG, and (e) 20% CRG

impact to the dissolution testing.

Elemental Analysis by ICP-OES

Potassium Ion (K^+) Release

Figure 9 show the potassium ion (K^+) release for duration of 13 weeks. The control sample (0% CRG) show the rapid release of K^+ while 5% CRG sample show moderate release (~1,200 ppm) at week 13. For higher CRG content (10-20%) demonstrated value for 700 ppm, 360 ppm, and 480 ppm. For K^+ release in control sample (0% CRG) show rapid release because of open porous glass and dissolved easily in deionized water same as conventional soluble fertilizer[24]. For 10% CRG show optimal K^+ release for 13-weeks and this matches plant growth perfectly which prevent the potassium from wasting in the soil but still manage the crops get enough nutrients for entire growing season[25].

Aluminium ion (Al^{3+}) release

All samples exhibited comparatively low Al^{3+} concentrations (<120 ppm at week 13), as shown in Figure 10. The control (0% CRG) had the lowest Al emission, approximately 70 ppm at week 13. Intermediate CRG levels (5-15%) exhibited a marginal increase in Al^{3+} release, due to the partial

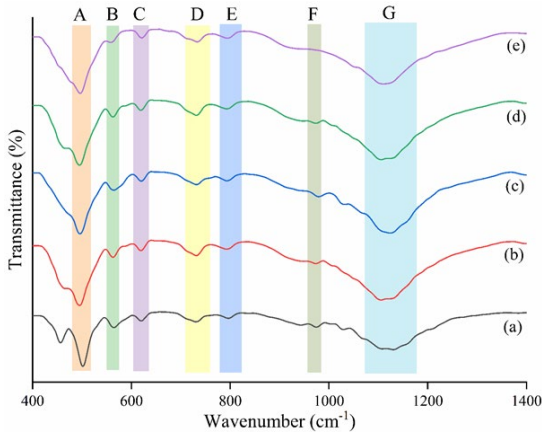

Fig. 4: FTIR Analysis for 5 different CRG-GF samples: (a) 0% CRG, (b) 5% CRG, (c) 10% CRG, (d) 15% CRG, and (e) 20% CRG

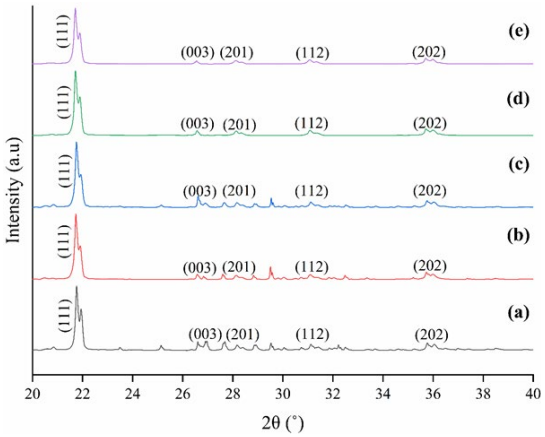

Fig. 5: XRD Analysis of CRG-GF samples: (a) 0% CRG, (b) 5% CRG, (c) 10% CRG, (d) 15% CRG, and (e) 20% CRG

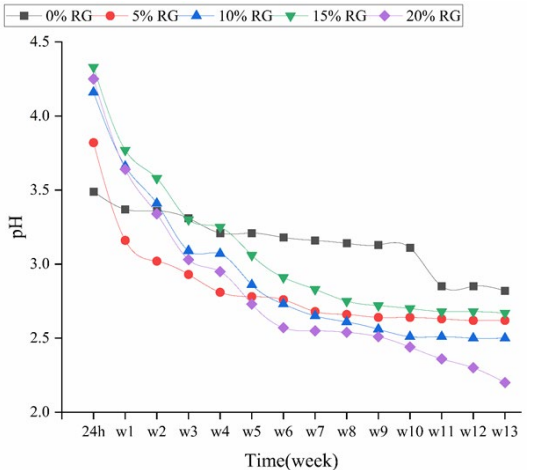

Fig. 6: pH levels of CRG-GF samples for 13-week dissolution in deionized water

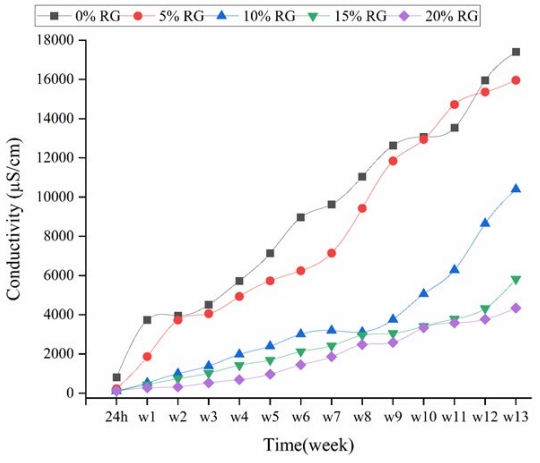

Fig. 7: Electrical Conductivity of CRG-GF samples over 13-week of dissolution in deionized water

breakdown of the aluminosilicate network caused by Fe^{3+} incorporation. The 20% CRG sample exhibited a significant late-stage increase post-week 9, indicating progressive degradation of the iron-aluminium crystalline phases and implying a two-phase dissolution process. For Al^{3+}, aluminium's role act as a network former that forms strong Al-O-Si and Al-O-P bonds [26]. From an agricultural perspective, the observed Al^{3+} release rates are formulated to be plant-safe. In acidic soil, regulated Al^{3+} release may potentially stabilize phosphate and regulated pH[27].

Iron ion (Fe^{3+}) release

Figure 11 show the iron ion (Fe^{3+}) release for 13-week dissolution testing and analyse using ICP-OES. The control sample (0% CRG) exhibited minimal Fe^{3+} leakage (~70 ppm) probably due to trace iron impurities. The 5% and 10% CRG samples exhibited moderate, steady Fe^{3+} release (90-150 ppm by week 13). For higher CRG (15% and 20%) release two type of pattern which initial burst release and accelerated release after week 9 and 10 (>280 ppm for 10% CRG). For last Fe^{3+} observed in this study because of iron is a vital micronutrient for chlorophyll synthesize and enzymatic functions in plants, and

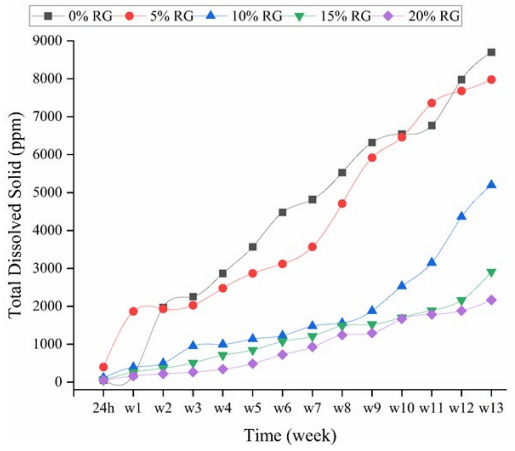

Fig. 8: TDS analysis from CRG-GF samples for 13 weeks of static dissolution in deionized water

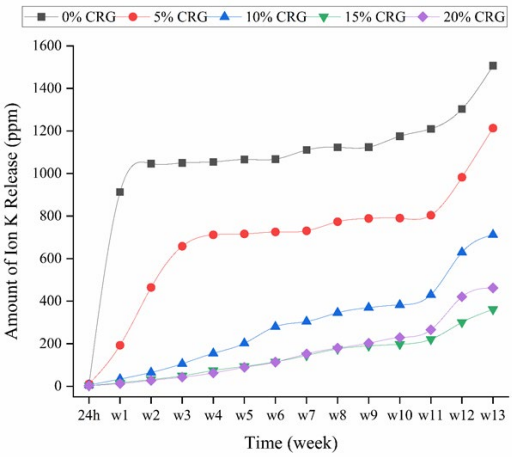

Fig. 9: Potassium (K^+) release from CRG-GF samples (0-20% CRG) during dissolution as determined by ICP-OES

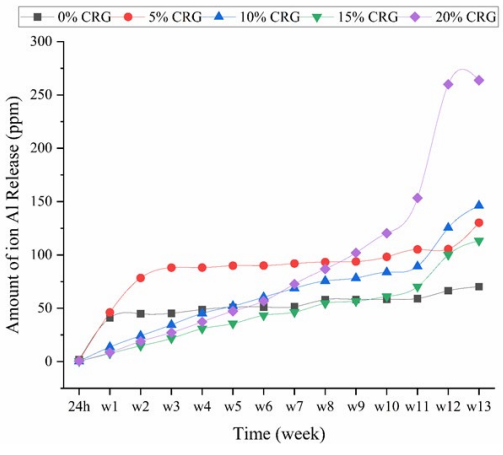

Fig. 10: Aluminium (Al^{3+}) release from CRG-GF samples (0-20% CRG) during 13-week dissolution as determined by ICP-OES

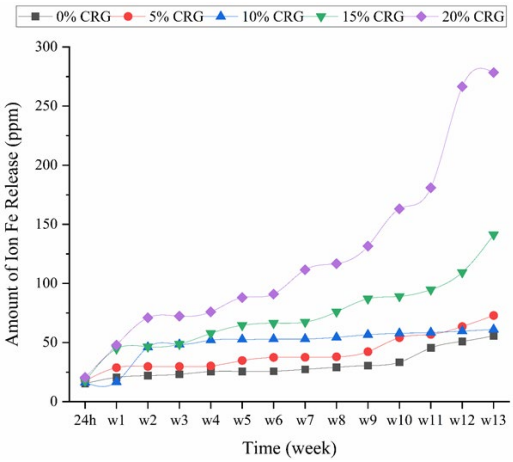

Fig. 11: Iron ion (Fe^{3+}) release of CRG-GF samples (0-20%) for 13-week dissolution a determined by ICP-OES

a critical element introduced by CRG substitution [28]. 10% CRG samples exhibited moderate, steady Fe^{3+} release demonstrate appropriate for sustained micronutrient enrichment and consistent with Fe^{3+} being effectively incorporated into the glass matrix rather than existing as easily leachable surface coatings[29].

CONCLUSION

In conclusion, this study is successfully investigated phosphate-silicate glass fertilizer with incorporating 0-20 wt.% of CRG by replacing CaO in glass system. Overall result in this study showed that increase of CRG made the structure of glass become denser and more crystalline but still maintaining the stability of the phosphate-silicate network. From dissolution testing over 13-weeks, the nutrient release shows the incorporation CRG influence how quickly nutrients were released. Low CRG content show rapid nutrient release, while higher content of CRG slow release because of glass structure.

The 10 wt.% CRG showed the best performance among all the CRG-GF formulations. This is because it showed a 53% reduction in K^+ compared to the control sample and a sustained release of K^+ (~700 ppm), Fe^{3+} (~150 ppm) and Al^{3+} (below 120 ppm), which are still at the safe levels for plants needed for 13-week study. In addition, 10% CRG demonstrated good nutrient-release performance which this formulation gives a practical way to recycle the RG byproduct, non-hazardous industrial waste (SW205), valorize it into safe and value-added in agricultural fertilizer. Future studies need to focus on field testing and long-term toxicity tests to confirm the glass fertilizer efficiency and safety for actual farming conditions.

ACKNOWLEDGEMENTS

The authors would like to thank the Faculty of Science and Marine Environment, Universiti Malaysia Terengganu (UMT), for providing laboratory facilities and technical support. The authors also acknowledge all staff and colleagues for the assistant and support throughout this research.

Conflict of Interest

The authors do not have any conflict of interest.

Funding Source Statement

This research was supported by the Ministry of Higher Education, Malaysia financial support of Fundamental Research Grant Scheme (FRGS) with Grant No. FRGS/1/2023/STG05/UMT/02/11

Authors' Contributions

Fatin 'Aqilah Mazlan contributed for conducted the experiments, analyzed data, and preparing the manuscript. Mohd Al Amin Muhamad Nor (Orcid Id: 0000-0001-8445-3776) contributed for supervised the research, reviewed the manuscript, and acts as corresponding author. Mazidah Mamat (Orcid Id: 0000-0002-3667-6243) and Mohd Faiz Hassan (Orcid Id: 0000-0002-8053-1973) contributed for data analysis and manuscript revision. All authors read and approved the final manuscript.

Data Availability Statement

The data findings in this study are available from the corresponding author upon reasonable request.

Ethical Approval Statement

Not applicable. This study did not involve human and animals.

Informed Consent Statement

Not applicable

REFERENCES

1. Shaviv, A.; Mikkelsen, R. L. Controlled-release fertilizers to increase efficiency of nutrient use and minimize environmental degradation – A review. *Fertilizer Research.* **1993**, *35*, 1-12
2. Vejan, P.; Khadiran, T.; Abdullah, R.; Ahmad, N. Controlled release fertilizer: A review on developments, applications and potential in agriculture. *Journal of Controlled Release.* **2021**, *339*, 321-334
3. Mohamad, S. H.; Nor, M. A. A. M. Effect of K_2O contents on the releasing of nutrient ions from phosphate glass system. *Key Engineering Materials*. **2017**, *723*, 545-550
4. Muhamad Nor, M. A. A.; Mohamad, S. H. Effect of Na_2O and K_2O on the solubility and chemical properties of P_2O_5 – CaO – Na_2O –

$K_2O – Al_2O_3$ glass. Materials Science Forum. 2017, 888, 146-150
5. Muhamad Nor, M. A. A.; Mohamad, S. H. Effect of Fe_2O_3 contents on the ions release from phosphate-based glass. *Materials Science Forum*. **2016**, *840*, 29-33
6. Labbilta, T.; Ail-El-Mokhtar, M.; Anli M.; Boutasknit A.; Abouliatim Y.; Khouloud M.; Meddich A.; Mesnaoui M. Controlled release fertilizers from phosphate glass-matrix: A new ecological approach to match nutrients release with plant demand. Boletin de la Sociedad Española de Cerámica y Vidrio. **2023**, *62*, 571-587
7. Mahazam, N.B.; Syafiqah, N.; Azmi, B. M. Evaluation of physical and chemical properties of red gypsum from Terengganu, Malaysia. *International Journal of Engineering Research and Technology.* **2016**, *5*, 433-436
8. Fauziah, I.; Zauyah, S.; Jamal, T. Characterization and land application of red gypsum: A waste product from the titanium dioxide industry. *Science of The Total Environment*. **1996**, *188*, 243-251
9. Gazquez, M. J.; Bolivar, J. P.; Vaca, F.; García-Tenorio, R.; Caparros, A. Evaluation of the use of TiO_2 industry red gypsum waste in cement production. *Cement and Concrete Composites.* **2013**, *37*, 76-81
10. Fauziah, C.I.; Hanani, M.N.; Zauyah, S.; Samsuri, A. W.; Rosazlin, A. Co-application of red gypsum and sewage sludge on acidic tropical soils. *Communications in Soil Science and Plant Analysis*. **2011**, *42*, 2561-2571
11. Azdarpour, A.; Karaei, M. A.; Hamidi, A.; Mohammadian, E.; Honarvar, B. CO_2 sequestration through direct aqueous mineral carbonation of red gypsum. *Petroleum*. **2018**, *4*, 398-407
12. Mohd, M. H.; Zuhamimi, N. A. S.; Saud, A.S.; Madduluri V. R.; Alshammari, H.; Maniam, G. P. Synthesis of glycerol carbonate from industrial by-products by alcoholysis of urea: Crude glycerol and red gypsum. *Fuel***.** **2024**, *357*, 129774
13. ASTM C373-14. Standard test method for water absorption, bulk density, apparent porosity, and apparent specific gravity of fired whiteware products, ceramic tiles, and glass tiles. *ASTM International: West Conshohocken, PA, USA*. **2014**, 1-5
14. Ersundu, M.C.; Kusu, B.; Ersundu, A.E. Structural properties and dissolution behavior of new generation-controlled release phosphate glass fertilizers. *Journal of Non-Crystalline Solids.* **2022**, *576*, 121239
15. Chen, M.; Liu, J.; Wu, Z. Effect of Fe_2O_3 concentration on the properties of basalt glasses. *Journal of Natural Fibers*. **2020**, *19*, 575-585
16. Sun, Y.; Zhang, Z.; Liu, L.; Wang, X. FTIR, Raman and NMR investigation of $CaO – SiO_2 – P_2O_5$ and $CaO – SiO_2 – TiO2 – P_2O_5$ glasses. *Journal of Non-Crystalline Solids*. **2015**, *420*, 26-33
17. Wu, H.; Feng, Y.; Li, H.; He, S.; Bian, Z. Red gypsum utilization and acidic wastewater treatment based on metal self-enrichment process. *Science of the Total Environment.* **2019**, *691*, 9-15
18. Kumar, B. Phosphate glasses and glass-ceramic for biomaterials. *Transactions of the Indian Ceramic Society***. 1985**, *44*, 123-127
19. Sitarz, M. Influence of modifying cations on the structure and texture of silicate-phosphate glasses. *Journal of Molecular Structure*. **2008**, *887*, 237-248
20. Massera, J.; Mayran, M.; Rocherullé, J.; Hupa, L. Crystallization behavior of phosphate glasses and its impact on the glasses' bioactivity. *Journal of Materials Science.* **2015**, *50*, 3091-3102
21. Kiwsakunkran, N.; Chanthima, N.; Kaewkhao, J.; Sangwaranateec, N. Composition and structural studies of glass fertilizer. *Journal of Physics: Conference Series*. **2018**, *1120*, 12016
22. Cheng, K. L.; Zhu, D. M. On calibration of pH meters. *Sensors*. **2005**, *5*, 209-219
23. Pan Liu, H.; Feng Huang, X.; Ping Ma, L.; Li Chen, D.; Shang, B.; Jiang, M. Effect of Fe_2O_3 on the crystallization behavior of glass-ceramics produced from naturally cooled yellow phosphorus furnace slag. *International Journal of Minerals, Metallurgy and Materials.* **2017**, *24*, 316-323
24. El-Damrawi, G.; Hassan, A. K.; Shahboub, A. Characteristic studies on $Ag_2O – Al_2O_3 – P_2O_5$ glasses and glass ceramics. *Materials Science and Engineering.* **2021**, *264*, 114957
25. Oosterhuis, D. M.; Loka, D. A.; Kawakami, E. M.; Pettigrew, W. T. The physiology of

potassium in crop production. *Advances in Agronomy*. **2014**, *126*, 203-233

26. Hruška, B.; Chromčíková, M.; Nowicka, A.; Macháček, J.; Gombárová, J.; Liška, M. Thermodynamic model and structural analysis of borosilicate glasses for pharmacy. *Journal of Thermal Analysis and Calorimetry,* **2025**, DOI: 10.1007/S10973-025-14932-Z.
27. Haynes, R. J.; Mokolobate, M. S. Amelioration of Al toxicity and P deficiency in acid soils by addition of organic residues: A critical review of the phenomenon and the mechanism involved. *Nutrient Cycling in Agroecosystems.* **2001**, *59*, 47-63
28. Morrissey, J.; Lou Guerinot, M. Iron uptake and transport in plants: The good, the bad, and the ionome. *Chemical Reviews.* **2009**, *109*, 4553-4567
29. Schmidt, W. Mechanism and regulation of reduction-based iron uptake in plants. *New Phytologist.* **1999**, *141*, 1-26.